3D Numerical study on the hollow profile polymer extrusion forming based on the gas-assisted technique

Z Ren[1,2,3], X Y Huang[2] and H S Liu[2]

[1]Key Laboratory of Optic-Electronic and Communication, Jiangxi Science and Technology Normal University, Nanchang, 330038, China
[2]School of Mechanical and Electrical Engineering, Nanchang University, Nanchang, 330031, China

E-mail: renzhong0921@163.com

Abstract. In this study, gas-assisted extrusion method was introduced into the extrusion of the hollow profiles. To validate the feasibility of the new extrusion method, 3D numerical simulation of the hollow profiles based on gas-assisted technique was carried out by using the finite element method. The Phan-Thien-Tanner (PTT) mode was selected as the construction equation. In the simulations, the physical field distributions of four different extrusion modes were obtained and analyzed. Results showed that the extrudate effect of traditional no gas-assisted mode was poor because the extrudate swell phenomenon is obvious and the physical field values are larger. For the gas-assisted of the inner wall, the extrudate swell of the melt was more obvious than that of the traditional no gas-assisted mode on account of the no-slip boundary condition on the outer wall. For the gas-assisted of the outer wall, the dimple effect of the inner wall is more obvious owing to the no-slip boundary condition on the inner wall. However, the extrusion effect of the double walls gas-assisted mode is very good because of the full-slip effect on the both walls.

1. Introduction

During the process of using plastic products, the hollow profiles [1, 2] are usually used in many fields, the engineering fields in particular, for example, architectural decoration, doorframe, etc. In general, the hollow profiles are made from the process of polymer melt extrusion. Due to the high viscosity of the melt, the high shear rate, shear stress and tensile stress in the die channel, the hollow profiles are easily distorted, such as the extrudate swell [3], the great deformation [4], and the melt fracture [5]. Up to now, the extrusion forming of the hollow profiles have been studied by some researchers, for example, Mu et al. [6, 7] used the finite element method and the differential multimode Phan-Thien and Tanner (mPTT) constitutive model to study the extrudate swell behavior of the hollow profiles. Zhang et al.[8] employed the finite element method to reversely predict and design the geometric structure of the die for the hollow profiles. Alfaro et al. [9] made use of the natural element method to study the extrusion behavior of the hollow profiles. However, the studies on the L-typed hollow profiles are very few. In this paper, to ascertain the mechanism of the extrusion deformation for the hollow profiles, the extrudate swells of the L-typed hollow profiles were studied through the finite element method. Moreover, to overcome the extrudate deformation of the L-typed hollow profiles, the gas-assisted extrusion technique was introduced and applied to the L-typed hollow profiles. To validate the feasibility of the gas-assisted extrusion technique, the numerical studies of four different

extrusion modes were analyzed and compared with each others from the physical field distributions, such as velocity, pressure, shear rate, and normal stress.

2. Numerical model and method

2.1. Geometric model

The geometric model and the finite element mesh of the L-typed hollow profiles are shown in Figure 1(a) and (b), respectively. In Figure 1(a), the face of $ABCDEF-A'B'C'D'E'F'$ is the inlet face of the die, the face of $HIJKLM-H'I'J'K'L'M'$ is the outlet of the die, the face of $NRSTUV-N'R'S'T'U'V'$ is the exit of the melt. The length of the inside die is about 30 mm, the length of the outside die is also about 30 mm, the high of AF is 30 mm, the wide of EF is 20 mm, the thickness of the hollow profile is 3 mm, and the width of the hollow part is 4 mm.

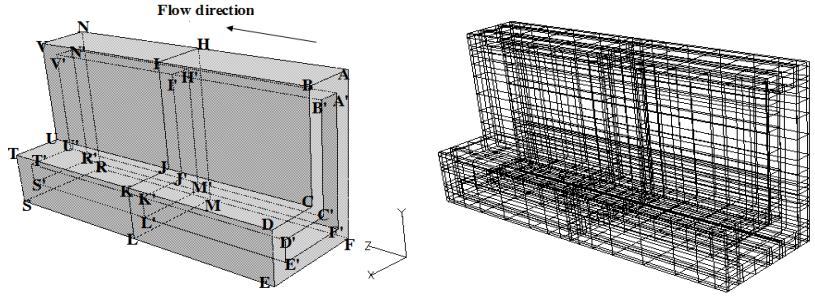

(a) geometric model (b) finite element mesh

Figure 1. Geometric model and mesh of the L-typed hollow profiles

2.2. Governing equations

In the numerical simulations, the polymer melt is regarded as the non-compressible, iso-thermal, steady, laminar and viscoelastic Non-Newtonian fluid. The gas is considered as the compressible, iso-thermal, steady, laminar and Newtonian fluid. Both the inertia, the gravity force, and the viscous dissipation effects and the diffuse effect of the gas enters into the melt all could be neglected.

The mass and the momentum equations are as follows:

$$\nabla \cdot v = 0 \tag{1}$$

$$-\nabla p + \nabla \cdot \tau = 0 \tag{2}$$

Where ∇ is Hamilton operator, v is the velocity of melt, p is the pressure drop, τ is the extra stress tension.

In this paper, PTT constitutive model [10] was used because it not only described the characteristic of the shear-thinning, but also represented the elastic properties of the viscoelastic fluid. PTT constitutive equation is as follows:

$$\exp\left[\frac{\varepsilon\lambda}{(1-\eta_r)\eta}tr(\tau_1)\right]\tau_1+\lambda\left[\left(1-\frac{\xi}{2}\right)\overset{\nabla}{\tau_1}+\frac{\xi}{2}\overset{\Delta}{\tau_1}\right] = 2(1-\eta_r)\eta D \tag{3}$$

where $\eta_r=\eta_2/\eta$ is the viscosity ratio, η is the total viscosity of the melt, η_2 is the Newtonian viscosity component of the melt, λ is the relaxation time, ε and ξ are the parameters of the melt correlated with the material tensile and the shear characteristics, respectively. $\overset{\nabla}{\tau_1}$ is the upper convected derivative of the extra stress tensor τ_1, η_1 is the Non-Newtonian component viscosity of the melt, and D is the strain-rate of the tensor.

In the simulations, for the PTT construction equation, its parameters can be seen from Table 1.

Table 1. The parameters of PTT construction equation

Parameters	η(Pa.s)	λ(s)	ε	ξ	η_r
Values	2700	0.2	0.18	0.23	0.12

2.3. Boundary conditions

- For the inlet face of the melt, the flow of melt is full-developed, steady and laminar flow, which is in accordance with the following relationship

$$\partial v_z / \partial z = 0, v_x = v_y = 0 \tag{4}$$

Where v_x, v_y and v_z are the flow velocities of melt at the direction of x, y and z direction, respectively.

- For the inner and outer wall of the mlet, no-slip wall boundary condition is suitable for the traditional no gas-assisted extrusion mode, which meets the following relationship,

$$v_n = v_s = 0 \tag{5}$$

But for the gas-assisted extrusion, the full-slip boundary condition is used meeting the following relationship,

$$v_s = 0, f_n = 0 \tag{6}$$

In this paper, the compressible air was used as the assisted gas in the gas-assisted polymer extrusion forming, and the temperature of gas should be heated to reach the temperature of the melt.

- For the free surface of the melt, zero normal stress and entangle velocity are imposed, the following equation should be expressed as following, i.e.,

$$f_n = 0,\ f_s = 0 \ \text{ and } \ v_n = 0 \tag{7}$$

- For the exit of melt, zero trance force and entangle velocity are imposed, i.e.,

$$f_n = 0,\ \ v_s = 0 \tag{8}$$

2.4. Numerical method

In this paper, the numerical simulations were carried out by using the finite element CFD software package POLYFLOW [11]. Because of the highly non-linear form of the differential viscoelastic constitutive equation used to describe material behavior, the position of the boundaries and free surface are unknown, and the position of the free surface becomes part of the solution, the nonlinear algebraic equation must be used to describe this class of problems, which result in the difficulties in solving the equations like the N-S equation. In order to solve these nonlinear equations, the coupled computing method of velocities-pressure was adopted. Since the total extra-stress tensor of differential constitutive equation was decomposed into the viscoelastic components and purely-viscous component, the elastic viscous split stress algorithm incorporating with the streamline upwind (EVSS-SU) algorithm [12] was used into the computing of the differential viscoelastic constitutive equations, and the momentum equations. And the implicit Euler discretization method [13] was incorporated into the integration of partial differential equations. In the interpolation scheme of finite element computing, the quadratic velocities, and linear pressure were used. For the free boundary and their moving-mesh problems, the coupled moving surface computing method and the Optimesh 3D remeshing method [14] were used. Moreover, to easily get the convergence solutions of the nonlinear equations, and the evolution schemes [11] of the material parameters, we also made use of boundary conditions and moving boundaries for instance, relaxation time of polymer melt, and the free boundary. In the convergence solving the nonlinear governing equations, the classical Newton-Raphson iterative algorithm [15] was used, the convergence condition is 1.0×10^{-4}.

3. Numerical results and analysis

3.1. X velocity distributions

To verify the feasibility of the gas-assisted extrusion method, the physical field distributions of four different extrusion modes are obtained, the X velocity distributions are shown in Figure 2.

From Figure 2(a), it is seen that the X velocity directions of two outer walls at the outlet of die are negative. The extrudate effect of traditional no gas-assisted extrusion method is poor, due to the extrudate swell effect, and the inner wall was adhered after the melt was extruded out from the die. From Figure 2(b), it is seen that the X positive velocities of two outer walls are very large, which result in the extrudate swell phenomenon being large. From Figure 2(c), it can be seen that the adhesion phenomenon is more obvious than that of the traditional no gas-assisted extrusion. However, as for the double gas-assisted extrusion mode, the extrudate effect is good, no extrudate swell and distortion phenomena occur on the extrudate because the velocity distribution of the melt at the outlet of the die is zero.

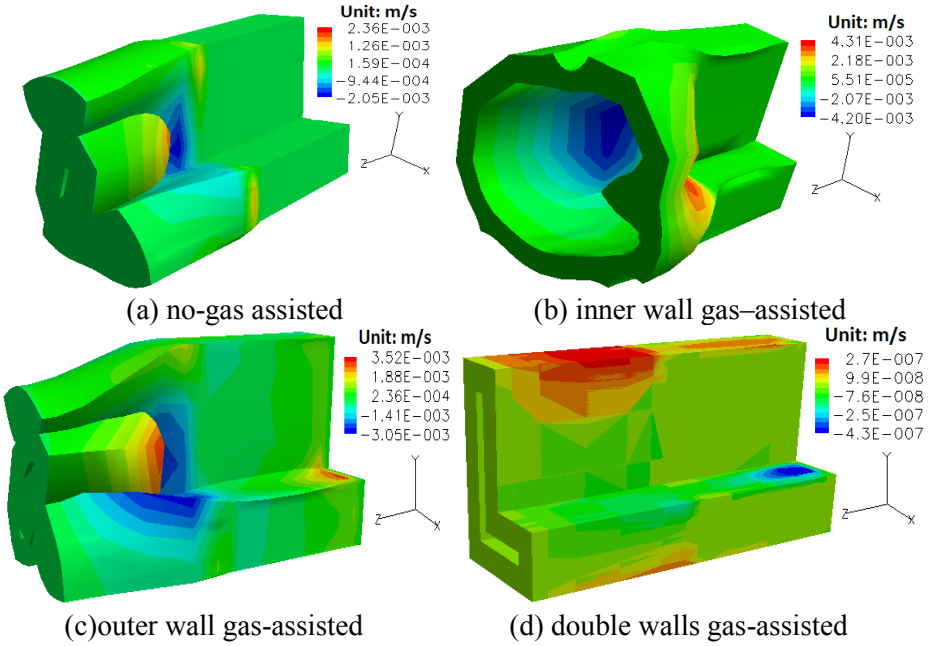

(a) no-gas assisted (b) inner wall gas–assisted

(c)outer wall gas-assisted (d) double walls gas-assisted

Figure 2. X velocity distributions of four different extrusion modes

3.2. Pressure distributions

From Figure 3, it is seen that the pressure gradient of traditional no gas-assisted extrusion mode is largest, which is the result of the no-slip wall boundary condition and the large flow resistance. But for the gas-assisted extrusion modes, it can be seen that the pressure gradients are decreased. In addition, for the double walls gas-assisted extrusion mode, the pressure gradient is very little, which leads to little extrusion deformation of hollow profiles.

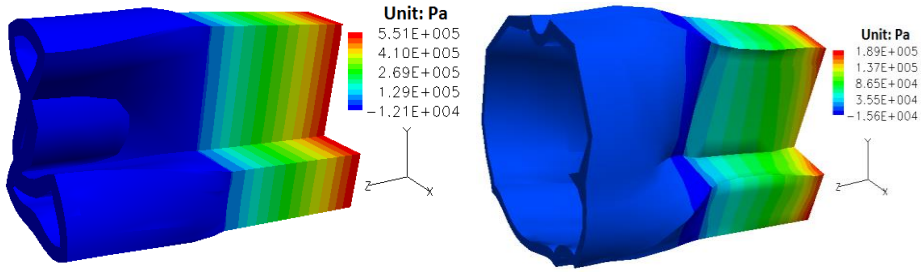

(a) no-gas assisted (b) inner wall gas –assisted

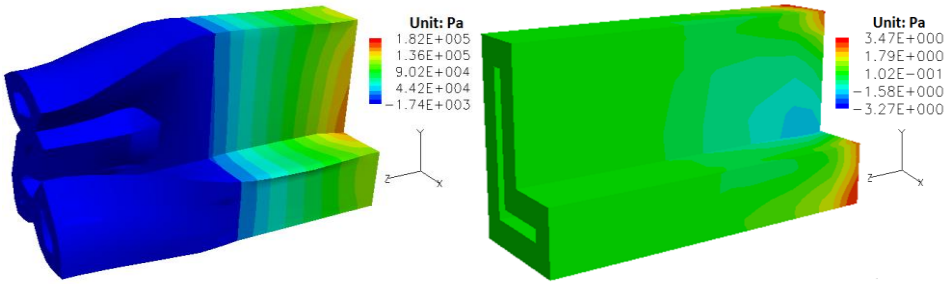

(c)outer wall gas-assisted (d) double walls gas-assisted

Figure 3. Pressure distributions of four different extrusion modes

3.3. Shear rate distributions

From Figure 4, it is seen that compared with others, the shear rate of no gas-assisted mode is the largest. As we all know, the larger both shear rate and velocity gradient are, the larger flow resistance is. While larger shear rate will result in larger shear stress on the wall of the die. But for the gas-assisted mode, the shear rates of melt are decreased, especially for the double walls gas-assisted mode.

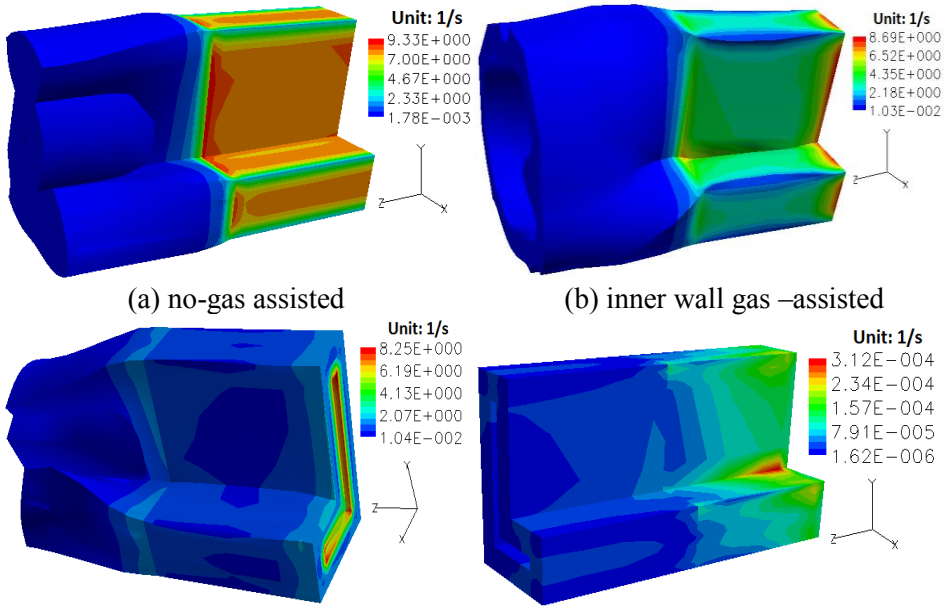

(a) no-gas assisted (b) inner wall gas –assisted

(c)outer wall gas-assisted (d) double walls gas-assisted

Figure 4. Shear rate distributions of four different extrusion modes

3.4. Normal stress distributions

As we know, the extrudate swell of the melt is related to the normal stress. To study the mechanism of overcoming the extrudate swell for gas-assisted extrusion mode, the first normal stress distributions of four different extrusion modes were obtained, which are shown in Figure 5 from which, it is seen that the first normal stress is large at the outlet of the die. However, for three kinds of gas-assisted extrusion mode, the first normal stress decreased. And for the double gas-assisted mode, the first normal stress is very little, which is so little that it can be neglected, which in return results in the elimination of the extrudate swell phenomenon for the hollow profiles.

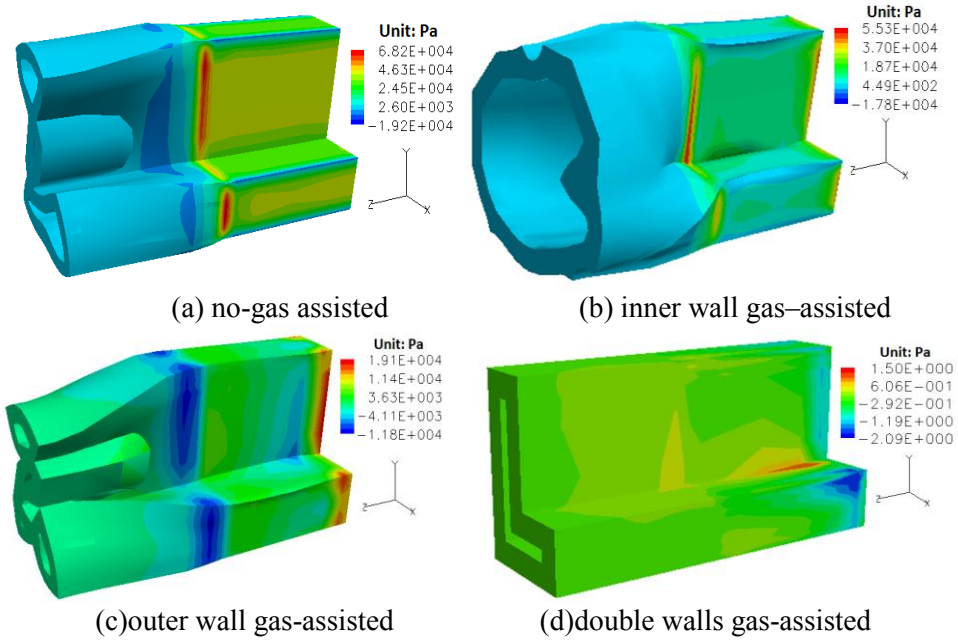

(a) no-gas assisted (b) inner wall gas–assisted

(c)outer wall gas-assisted (d)double walls gas-assisted

Figure 5. Normal stress distributions of four different extrusion modes

4. Conclusions

Extrudate swell is a common phenomenon in the processing of polymer melt, which also occurs in the hollow profiles extrusion. To overcome the extrudate swell of hollow profiles, the gas-assisted mode was introduced and analyzed by using the numerical simulation method in the study. And to validate the feasibility of gas-assisted mode, the physical field distributions of four different gas-assisted modes were obtained and compared with others. Research results indicated that the extrusion effect of the traditional no gas-assisted mode is poor, the extrudate swell is obvious, and the inner wall is easily adhered. For the gas-assisted in single wall, for example, for the inner wall gas-assisted mode, the extrudate swell phenomenon of the melt was more obvious than that of the traditional no-gas assisted mode. For the outer wall gas-assisted mode, the adhesion effect was more obvious. However, as for the double walls gas-assisted mode, the extrudate swell and the deformation are all greatly eliminated. Therefore, the double wall gas-assisted technique has a potential value in the process of the hollow profiles.

Acknowledgements

This work is supported by the Natural Science Foundation Project of Jiangxi Province (No. 20151BAB202011), the Science and Technology Pillar Program Project of Jiangxi Province (No. 20132BBG70103), Top-notch Talent Foundation Project of JXSTNU (No. 2014QNBJRC004), and 2011 Cooperative Innovation Center Project of Jiangxi Province (No. 2014XTCX005).

References

[1] Reggiani B, Segatori A, Donati L, et al. 2014 Comparison of bulge test vs. conical expansion test for hollow extruded profile characterization. *Key Eng. Mater.* **585** 111-119

[2] Sun Y D, Chen Q R, Sun W J 2015 Numerical simulation of extrusion process and die structure optimization for a complex magnesium doorframe. *Int. J. Adv. Manuf. Tech.* **80** 495-506

[3] Konaganti V K, Ansari M, Mitsoulis E, et al. 2015 Extrudate swell of a high-density polyethylene melt: II. Modeling using integral and differential constitutive equations. *J.Non-Newton. Fluid Mech.* **225** 94-105

[4] Shibakov V G, Pankratov D L, Andreev A P, et al. 2015 Prediction of samples failure during severe plastic deformation by multiple extrusion. *IOP Conf. Ser.: Mater. Sci. Eng.* **86** 12032-12036

[5] Kwon Y 2015 Melt fracture modeled as 2D elastic flow instability. *Rheol. Acta* **54** 445-453
[6] Mu Y, Zhao G, Wu X, Zhai J 2013 Finite-element simulation of polymer flow and extrudate swell through hollow profile extrusion die with the multimode differential viscoelastic model. *Adv. Polym.Tech.***32** E1-E19
[7] Mu Y, Zhao G Q, Zhang C R 2010 Numerical investigation of viscoelastic flow and swell behaviors of polymer melts in the hollow profile extrusion process. *Adv. Mater.s Res.* **97-101** 209-213
[8] Zhang M, Huang C Z, Jia Y X, Liu J L 2014The inverse prediction for profile extrusion die based on the finite element method. *Adv. Mater.s Res.* **941-944** 2332-35
[9] Alfaro I, Gagliardi F, Olivera J, et al. 2009 Simulation of the extrusion of hollow profiles by natural element methods. *Int. J.Mater. Form.* **2** 597-600
[10] Thien N P, Tanner R I 1977 A new constitutive equation derived from network theory. *J.Non-Newton. Fluid Mech.* **2** 353-365
[11] ANYSYS Inc.2012 ANYSYS POLYFLOW Version 14.5 User's Guide. Canonsburg, PA, USA
[12] Sun J, Phan-Thien N P, Tanner R I 1996 An adaptive viscoelastic stress splitting scheme and its applications: AVSS/SI and AVSS/SUPG. *J.Non-Newton. Fluid Mech.* **65** 75-91
[13] He Y N 2013 Euler implicit/explicit iterative scheme for the stationary Navier–Stokes equations. *Numer. Math.* **123** 67-96
[14] Su Y Y, Rwei S P, Wu L Y, Lin Y T, An T C, Lin W P, Chien S P, Lin L Y 2011 Shaping conjugated hollow fibers using a four-segmented arc spinneret. *Polym. Eng. Sci.* **51** 704–711
[15] Caddemi S, Martin J B 1991 Convergence of the Newton-Raphson algorithm in elastic-plastic incremental analysis. *Int. J. Numer. Meth. Eng.* 66 71-76